Comparison of laser-based and conventional calibrations of sun photometers

Nordine Souaidia[a], Christophe Pietras[b], Giulietta Fargion[b], Robert A. Barnes[b], Robert Frouin[c]
Keith R. Lykke[a], B. Carol Johnson[a], and Steven W. Brown[a]

[a]*Optical Technology Division, National Institute of Standards and Technology, Gaithersburg, MD 20899, USA*

[b]*NASA SIMBIOS Project, Science Applications International Corporation, Beltsville, MD 20705, USA*

[c]*Scripps Institution of Oceanography, La Jolla, CA*

ABSTRACT

Sun photometers are used to characterize the radiative properties of the atmosphere. They measure both the incident solar irradiance as well as the sky radiance (from scattered incident flux). Global networks of sun photometers provide data products such as aerosol optical thickness derived from these measurements. Instruments are typically calibrated for irradiance responsivity by cross-calibration against a primary reference sun photometer and for radiance responsivity using a lamp-illuminated integrating sphere source. A laser-based facility for Spectral Irradiance and Radiance Responsivity Calibrations using Uniform Sources (SIRCUS) has been developed at the National Institute of Standards and Technology. Sensors can be calibrated in this facility for absolute spectral irradiance and radiance responsivity with combined expanded (k = 2) uncertainties ranging from 0.15 % to 0.25 %. Two multi-channel filter radiometers used in the Sensor Intercomparison and Merger for Biological and Interdisciplinary Oceanic Studies (SIMBIOS) program of the National Aeronautics and Space Administration (NASA) at the Goddard Space Flight Center (GSFC) were calibrated for radiance and irradiance responsivity using conventional approaches and using laser-illuminated integrating spheres on SIRCUS. The different calibration methods are compared, the uncertainties are evaluated, and the impact on remote sensing applications is discussed.

Keywords: Calibration, irradiance, radiance, responsivity, solar irradiance, sun photometer

1. INTRODUCTION

Ground-based measurements of the direct solar irradiance and the diffusely scattered solar radiance have been widely used to characterize the optical properties of the atmosphere and derive information about the composition and distribution of aerosols. More recently, global aerosol distributions have been measured remotely using satellite-borne sensors. The information derived from these measurements is used for aerosol research and radiative transfer modeling as required for global climate change studies. In satellite-based ocean color remote sensing measurements, approximately 90 % of the signal measured at the satellite sensor comes from atmospheric scattering. Proper atmospheric characterization and aerosol modeling is necessary to separate the atmospheric component from the top-of-the-atmosphere radiance, required for valid satellite-based measurements of ocean color data products such as global, near-surface, phytoplankton chlorophyll-*a* distributions.

Sun photometers and sky radiometers are used to characterize the optical properties of the atmosphere. Measurements are used to validate remote sensing aerosol optical thickness retrievals, evaluate current aerosol models and in the development of vicarious sensor calibration methodologies [1]. Networks of sun photometers are distributed globally through the National Aeronautics and Space Administration's (NASA's) Aerosol Robotic Network (AERONET) [2], NASA's Sensor Intercomparison and Merger for Biological and Interdisciplinary Oceanic Studies (SIMBIOS) Project [3] and the World Radiation Center (WRC), Davos, Switzerland [4]. Sun photometers make measurements of the direct solar irradiance as well as the sky radiance. These are distinct radiometric measurements and instruments are typically calibrated for both irradiance and radiance responsivity. Instruments are calibrated for radiance

responsivity using lamp-illuminated integrating sphere sources (ISSs). One such facility is the Radiometric Calibration Facility (RCF) at NASA's Goddard Space Flight Center (GSFC) [5]. The combined standard uncertainty in the absolute calibration of sky radiometers using lamp-illuminated integrating spheres at the RCF is approximately 5 % [6]. For irradiance responsivity, sun photometers are often calibrated by a Langley-Bouguer cross-calibration technique against a primary reference sun photometer [6]. For AERONET and SIMBIOS sun photometer networks, for example, the reference sun photometers are calibrated using the Langley-Bouguer technique at Mauna Loa Observatory, Hawaii [2]. The calibration consists of determining the signal, V_o, from the sun photometer in the absence of atmospheric scattering. Instruments deployed in the network are calibrated at NASA's Goddard Space Flight Center by cross-calibration against the primary reference instruments. The combined standard uncertainty in the calibration is approximately 3 %.

Improvements in the radiometric accuracy of sun photometers used for atmospheric characterization will enable better modeling of global aerosol distributions and reduce the error in ocean color measurements by better correcting for the effects of aerosols on the total radiance recorded by the satellites [7]. Schmid, et al., [8] compared the results of a Langley-Bouguer calibration with a laboratory calibration using a standard irradiance lamp and a number of different exo-atmospheric solar irradiance models. They discussed the effects of wavelength error, finite bandpass, and spectral out-of-band contribution, and evaluated the components for optimal conditions: solar calibrations at high altitude and use of NIST-traceable irradiance lamps. The relative expanded uncertainty ($k = 2$) in the Langley-Bouguer calibration was 1 % or less for atmospheric channels with no strong absorption features from 450 nm to 1024 nm, increasing to 1.35 % at 412 nm. The combined expanded uncertainties ($k = 2$) in the standard lamp calibrations, including 1.3 % uncertainty in the lamp irradiance, a 0.4 % experimental uncertainty, and a 0.75 % uncertainty in the sun photometer relative spectral responsivity, were approximately 1.5 % over the same spectral range. With the uncertainty in the exo-atmospheric solar irradiance spectrum included, the combined expanded uncertainty in the laboratory calibration was between 2 % and 4 %, or a factor of 2 to 4 larger than the Langley-Bouguer calibration.

Reductions in the calibration uncertainties of sun photometers using laboratory standards would allow for meaningful comparisons with the results from the solar-based calibration (Langley-Bouguer method), resulting in independent values for the exo-atmospheric solar irradiance at the set of measurement wavelengths [8, 9]. Laboratory calibrations using SIRCUS (see below) or standard radiometric artifacts (e.g. FEL-type standard irradiance lamps) provides traceability to SI units, and is useful for world-wide intercomparisons and validation of instrument uncertainties. A newly developed laser-based facility for Spectral Irradiance and Radiance Responsivity Calibrations using Uniform Sources (SIRCUS) at the National Institute of Standards and Technology (NIST) is ideally suited for both radiance and irradiance responsivity characterizations and calibrations [10, 11]. The irradiance from the ISS at a reference plane can be determined with an expanded uncertainty ($k = 2$) of approximately 0.1 %. (Similarly, the radiance of the laser-illuminated ISS can be determined with an expanded uncertainty ($k = 2$) of approximately 0.2 %). Consequently, with the development of the SIRCUS facility, we are in a position to significantly reduce the uncertainty in the laboratory calibration method compared to that reported by Schmid, et al. [8].

In this work, we discuss the calibration of two similar radiometers, the Satellite Validation for Marine Biology and Aerosol Determination (SimbadA) radiometers (serial numbers 07 and 09), manufactured by the Laboratoire d'optique atmospherique (LOA) de Lille[1], France. The SimbadA are eleven-channel filter radiometers with nominal channel center wavelengths at 350 nm, 380 nm, 410 nm, 443 nm, 490 nm, 510 nm, 565 nm, 620 nm, 670 nm, 750 nm and 870 nm, respectively. The radiometers are operated by NASA's Sensor Intercomparison and Merger for Biological and Interdisciplinary Oceanic Studies (SIMBIOS) Program. Several instrument channels were calibrated for both radiance and irradiance responsivity using laser-based ISS on the SIRCUS facility. The radiance responsivity results were compared with calibrations using two lamp-illuminated ISSs of known spectral radiance: the primary calibration source at the RCF facility at NASA's GSFC, known as the Hardy source, [6] and a NASA lamp-illuminated ISS maintained by NIST known as the NIST Portable Radiance (NPR) source [12]. The laser-based irradiance responsivity calibrations are compared with the cross-calibration against a primary reference sun photometer using exoatmospheric solar irradiance models by Thuillier [13], Neckel and Labs [14], MODTRAN [15], and Wehrli [16].

Results were similar for the two instruments; details for instrument 09 are presented below. A description of the measurements is given in Section 2, and the results from the radiance and irradiance responsivity calibrations are described in Section 3.

---

[1] Certain commercial equipment, instruments, or materials are identified in this paper to foster understanding. Such identification does not imply recommendation or endorsement by the National Institute of Standards and Technology, nor does it imply that the materials or equipment are necessarily the best available for the purpose.

2. EXPERIMENTAL

2.1 The NIST SIRCUS Facility

A schematic of the SIRCUS facility is shown in Fig. 1. A number of tunable laser systems are used to generate light over a wide spectral range; this work focused on the region from 420 nm to 900 nm. The output of the laser is stabilized to reduce the magnitude of intensity fluctuations and a portion of the beam is directed to a wavemeter for determination of the wavelength. The main portion of the beam is input to the integrating sphere using an optical fiber. The effect of speckle, which introduces noise in the radiometric measurements, is reduced by placing a small length of the optical fiber in an ultrasonic bath. A monitor detector corrects for small fluctuations in the radiant flux during a calibration. The SIRCUS ISS is a uniform, monochromatic, high-flux, Lambertian source of known radiance.

Test sensors and a reference primary standard detector are located on a translation stage at a fixed (and known) distance from the sphere exit aperture. The test sensors are calibrated against the reference detector using the substitution method. A computer program controls and monitors the laser power and wavelength, moves the translation stage, and records test and reference detector signals.

Integrating sphere sources are available with overall diameters from 2.5 cm to 50 cm. The size of the ISS and its exit aperture are selected to match the geometric requirements of the radiometer under test: smaller exit apertures, which under-fill the field-of-view of the radiometer, for irradiance characterizations and larger ones, which overfill the field-of-view of the radiometer, for radiance characterizations. For radiance responsivity calibrations, a 30 cm diameter integrating sphere with a 12 cm diameter exit port was used to determine the radiance responsivity. For irradiance responsivity measurements, a quasi-point source is preferred: a 2.5 cm diameter integrating sphere with a 1 cm diameter aperture was used.

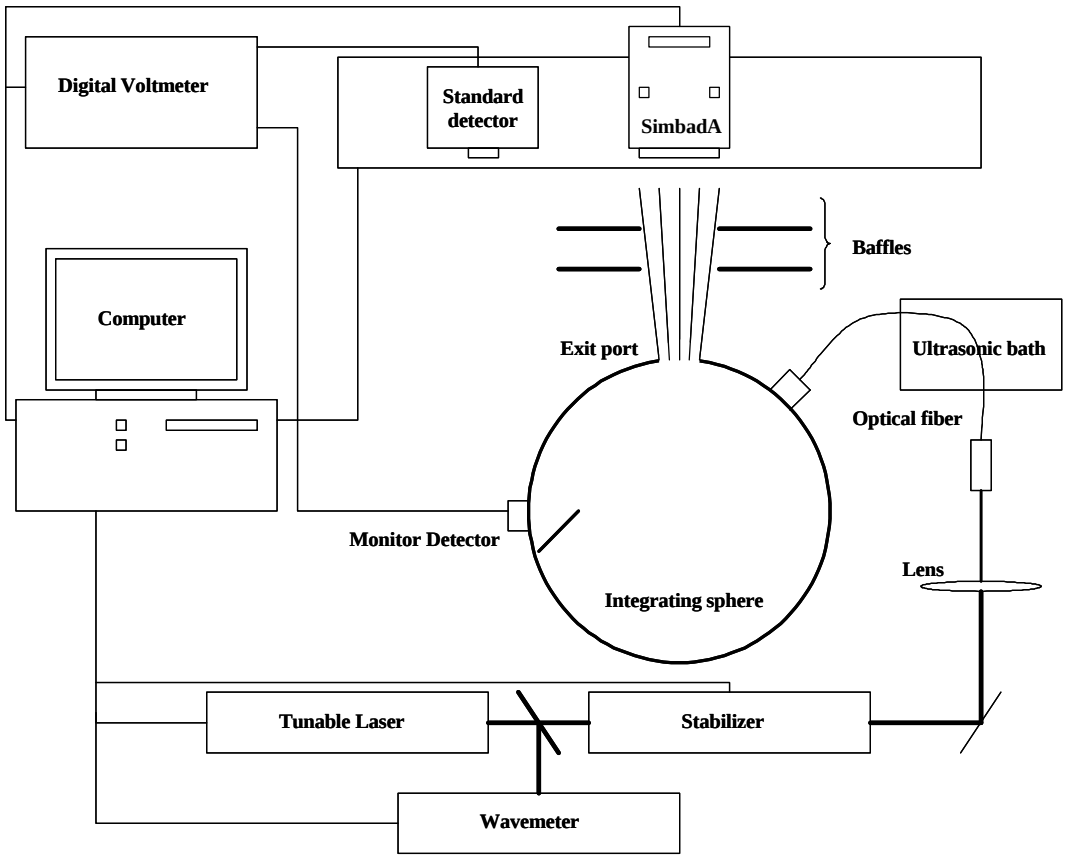

Figure 1: Schematic of the SIRCUS facility, illustrating the laser-illuminated integrating sphere, the standard detector, and the SimbadA.

The low uncertainties possible on SIRCUS stem from a number of unique characteristics of the laser-based calibration facility: the laser is monochromatic (with its wavelength determined interferometrically), high flux levels are possible, the entrance pupil of the sun photometer is filled according to the conditions of solar viewing, and there is no need for a standard lamp of spectral irradiance. The radiance of the source is determined using reference standard silicon transmission trap detectors [17]. The trap detectors were calibrated for spectral power responsivity directly against a cryogenic radiometer with uncertainties of 0.05 % or less. For irradiance measurements, a precision aperture was placed at the trap entrance port. The aperture area was measured on the NIST Aperture Area Facility with an uncertainty in the aperture area of 0.01 % [18]. Except for dependence on ambient temperature, pressure, and humidity, all uncertainty components related to the laboratory radiometer are quantified, so systematic effects can be eliminated. To validate the uncertainties, a pyrometer was calibrated for absolute spectral radiance responsivity on SIRCUS. The pyrometer then measured the radiance of a gold-melting point and a silver-melting-point blackbody. The predicted signals, based on Planck's law (given the temperature of the metal melting point) and the absolute spectral responsivity of the pyrometer, agreed with the measured signals to within 0.2 % for the gold-melting-point blackbody and within 0.1 % for the silver-melting-point blackbody [19].

2.2 NASA's RCF Integrating Sphere Source

To reduce particulate contamination, the RCF is located in an ISO Class 7 (Class 10000) clean room. The primary calibration source in the RCF is a 1.8 m diameter fiberglass-shelled, lamp-illuminated ISS known as Hardy. The Hardy sphere is a fan-cooled fiberglass shell with a barium sulfate ($BaSO_4$) interior coating. The sphere exit aperture is 25.4 cm. The sphere is equipped with 16 individually baffled 200 W quartz tungsten halogen lamps. Eight 500 W power supplies power pairs of lamps in a constant current mode. Hardy is used in the RCF to calibrate sun photometers that are part of global networks of *in situ* atmospheric characterization and to calibrate other radiometers that are employed in the validation of EOS satellite instruments. During operation, the sphere output was monitored at six channels using a new Filter Radiometer Monitoring System (FRMS) [20]. The FRMS, which has a filter wheel for observation at discrete wavelengths, mounts to Hardy above the exit aperture and looks at the radiance from the back wall of the sphere opposite the exit port. The center wavelengths of the filters are 410 nm, 440 nm, 460 nm, 640 nm, 840 nm, and 1050 nm.

Hardy is calibrated monthly using a single grating, scanning monochromator (model OL746 from Optronic Laboratories, Inc.) operating in the irradiance mode; this configuration is known as the 746/ISIC (integrating sphere irradiance collector). Lamp standards of spectral irradiance purchased directly from NIST were used to calibrate the 746/ISIC. The uncertainty in the spectral radiance of lamp-illuminated ISSs depends on the method used, the reference standard, the transfer standard, and the wavelength range. The relative expanded uncertainties ($k = 2$) for Hardy are approximately 2.5 % in the visible, increasing to 6.5 % at the 400 nm.

2.3 The NIST Portable Radiance Source

The NPR is a 30 cm diameter Spectralon™ sphere with a 10 cm diameter aperture. It was developed by NIST in collaboration with NASA's Earth Observing System Calibration/Validation Program Office [12]. The sphere is equipped with 4 internally baffled, 30 W lamps located at 90 degree intervals around the aperture. Two photodiodes are used in the sphere to monitor the sphere radiance: an Indium Gallium Arsenide (InGaAs) detector with an infrared filter centered at 1400 nm and a silicon detector with a photopic filter centered at 550 nm. The NPR was calibrated in the NIST Facility for Automated Spectral Irradiance and Radiance Calibrations (FASCAL) [21] against primary national radiometric standards. For the NPR, the relative expanded uncertainties ($k = 2$) are a factor of 5 lower than for Hardy, approximately 1.0 % in the ultraviolet (UV), 0.5 % in the visible, and 1.5 % in the short wave infrared (SWIR).

2.4 The Langley-Bouguer cross-calibration at NASA's GSFC

For irradiance measurements (e.g., solar-viewing), the SimbadA instruments are compared to reference sun photometers in a cross calibration technique on a rooftop at GSFC. The reference sun photometers, which are part of the AERONET project are calibrated at the Mauna Loa Observatory on regular intervals [6]. The cross calibration technique, described in Ref. [2], consists of near simultaneous solar observations at GSFC with the uncalibrated SimbadA instruments and the reference sun photometers. The method assumes that the ratio of the output voltages for

the same channel (e.g., same nominal relative spectral responsivity) for the reference and uncalibrated radiometers and a particular air mass is proportional to the ratio of the output voltage at zero air mass. If the spectral responsivities differ, a correction is made for spectral differences related to Rayleigh, ozone, and aerosol attenuation [6]. This process is sensitive to the accuracy and completeness of the spectral irradiance responsivity for each channel.

3. RESULTS

Prior to the calibration, the temporal stability and gain calibration of the instruments were evaluated. The temporal stability of the SimbadA's responsivity was evaluated on SIRCUS and with the NPR source. Measurements were made with and without a warm-up interval. The result was an observable drift of approximately 0.5 % in the instrument's responsivity during the first hour of use. The SimbadA instruments have two gain settings, one for solar measurements and one for sky or ocean measurements. Using the NPR, the gain ratio was measured and compared to the previous value in use by the SIMBIOS program. The values agreed to within 0.5 %. In Section 3.1, we discuss the radiance responsivity calibration comparison; the irradiance responsivity comparison will be discussed in Section 3.2.

3.1. Radiance responsivity comparison

Eight of the channels were studied in this work; no measurements were made for the 350 nm, 380 nm, and the 410 nm channels. Each channel's absolute spectral radiance responsivity was measured on SIRCUS approximately every 0.25 nm within ±15 nm of a channel's band-averaged center wavelength. This spectral range covered each channel's 'in-band' region, where the in-band region is defined as the region over which the responsivity is 0.1 % of the maximum channel responsivity or greater. The spectral out-of-band responsivity was measured using a lamp-monochromator system in the NIST Spectral Calibration Facility (SCF) [22]. For each channel, the out-of-band signal was 0.01 % of the maximum value or less over the spectral range from 380 nm to 1050 nm. A typical channel's absolute spectral radiance responsivity $s^i(\lambda)$ measured on SIRCUS is shown in Fig. 2. Interference fringes arising from multiple reflections were observed in the two longest wavelength channels. For the 870 nm channel, the magnitude of the fringes was approximately 10 %, as shown in Fig. 3.

The SimbadA instruments were calibrated with both the Hardy and the NPR sources (at NASA's GSFC and NIST, respectively) in May 2002. For each channel *i*, the band-averaged calibration coefficient, C_i, was calculated according to

$$C_i = Sig_i(DN) * \frac{\int s^i_{rel}(\lambda)\,d\lambda}{\int L(\lambda)\, s^i_{rel}(\lambda)\,d\lambda}, \qquad (1)$$

where $Sig_i(DN)$ is the net digital signal from channel *i*, in counts or digital number (DN); $L(\lambda)$ is the spectral radiance from either the Hardy or the NPR ISS; and $s^i_{rel}(\lambda)$ is the relative spectral responsivity (RSR) of channel *i*. The second term on the right hand side of Eq. 1 is the band-averaged radiance.

Prior to the SIRCUS measurements, the only information available to the SIMBIOS program for a channel's RSR was filter transmittance data from the instrument manufacturer. The RSR for each channel was then modeled assuming the detector response was constant over the bandpass. SIRCUS provided the first determination of the RSR for the complete system (obtained by simply normalizing the ASR). The difference between the manufacturer-supplied filter transmittance and the SIRCUS-derived spectral responsivity can be significant. The SIRCUS RSR for the 490 nm channel is shown in Fig. 4 along with filter transmittance results from the SimbadA manufacturer. Band-center wavelengths for each channel were calculated using both SIRCUS and manufacturer data according to:

$$\lambda^i_c = \frac{\int \lambda s^i_{rel}(\lambda)\,d\lambda}{\int s^i_{rel}(\lambda)\,d\lambda}. \qquad (2)$$

For this channel, the center wavelengths for the two approaches differ by 0.85 nm, with the SIRCUS results shifted to longer wavelengths. The band-center wavelength for each channel is listed in Table 1 using manufacturer and SIRCUS data for $s^i_{rel}(\lambda)$.

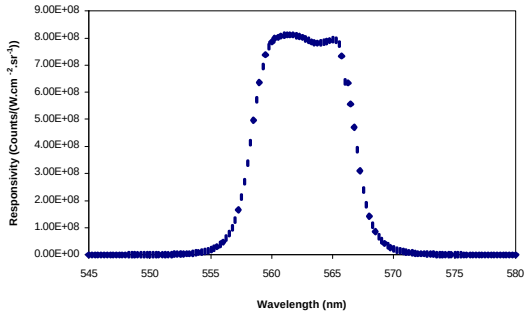

Figure 2: SimbadA channel 4's absolute spectral responsivity $s^4(l)$ measured on SIRCUS.

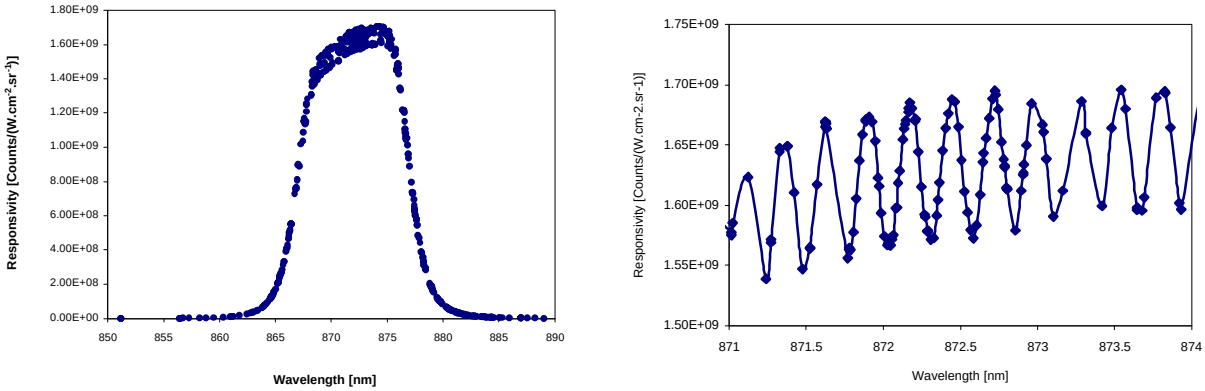

(a) (b)

Figure 3: (a) SimbadA channel 8's absolute spectral responsivity $s^8(\lambda)$ measured on SIRCUS. (b) Expanded view showing oscillations in the responsivity arising from multiple reflections of the incident radiation within an optical element of the filter channel.

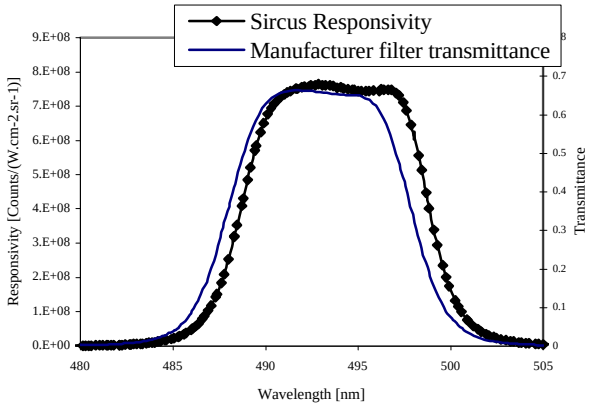

Figure 4: Absolute radiance responsivity of the 490 nm channel of SimbadA S/N 09 and manufacturer transmittance measurements.

	Band-Center Wavelength		$C_i(\ddot{e})$ [DN/(W/cm3/sr)]			
Channel	SIRCUS	Manf.	Sircus	Nipper	Hardy (manf. RSR)	Hardy (SIRCUS RSR)
1	443.74	442.72	745.6	750.9	791.9	781.8
2	493.77	492.74	812.5	816.8	861.7	853.7
3	511.98	510.72	892	856.4	897.5	888.9
4	562.56	562.17	726	724.4	756.4	754.3
5	622.19	622.68	1111.4	1104.1	1167.9	1168
6	672.56	672.19	1229	1232.8	1296.5	1295.2
7	752.55	752.56	1494.7	1498.4	1588.3	1588.4
8	872.4	871.38	1285.2	1320.0	1358.8	1359

Table 1 : SimbadA channel band center wavelengths and band-averaged responsivities derived from measurements of NPR and Hardy.

Because sun photometer calibrations at NASA's RCF with Hardy historically used manufacturer's RSR's, band-averaged calibration coefficients from the Hardy calibration were calculated using the two different data sets. For the NPR measurements, only the SIRCUS RSR's were used. In each case, radiance responsivities sphere spectral radiance values $L(l)$ were interpolated to a uniform wavelength interval of 0.25 nm to calculate C_i. Band-averaged responsivities are listed in Table 1. Note the 1 % difference in C_i*'s* for channels 1 through 3 when calculated using the two different sets of RSRs.

Typically when comparing with SIRCUS and lamp-illuminated ISS calibrations, the signals obtained when measuring a lamp-illuminated ISS such as Hardy or the NPR are compared to the predicted signals, where the predicted signal is given by:

$$Sig^{i}_{predicted}(DN) = \int L(l)\, s^{i}(l)\, dl \qquad (3)$$

In this case, because of the relatively narrow bandwidth of the filter channels (~ 10 nm) we define a SIRCUS-derived calibration coefficient to be:

$$C_i^{SIRCUS} = \int s^i(\lambda) d\lambda, \qquad (4)$$

where the integration extends over the in-band spectral region.

The difference between the two approaches is small, on the order of a couple of tenths of a percent. Results are listed in Table 2. The SIRCUS predicted signal agrees with the measured signal from NPR to within 0.3 % for SimbadA channels 4 through 7. The difference increases slightly for channels 1 and 2, rising to 0.7 % for channel 1. These results are in good agreement with previous comparisons between laser-based and lamp-illuminated ISS-based calibrations of transfer radiometers [23]. Two channels gave anomalous results: the SIRCUS predicted signal disagreed with the measured signal by 4.15 % for channel 3 and 2.64 % for channel 8. Large interference fringes arising from multiple reflections of the incident radiation within the channel were observed in the responsivity of channel 8 measured on SIRCUS (Fig. 3) and could be a cause of the observed difference. (Measuring the responsivity with finer spectral resolution would eliminate this potential source of error.) Examination of the SIRCUS data for channel 3 showed a 1.5 nm gap in the ASR data near 514 nm: no data were acquired over this spectral region. This could give rise to an error in the interpolation of the SIRCUS data to 0.25 nm spacing.

The Hardy measurements disagreed with SIRCUS and with NPR-derived responsivities by 2.5 % to 6 % by, depending on the channel. The observed differences are slightly larger than those measured during previous comparisons of NPR and Hardy radiances [24, 25]. For both comparisons, the difference in the measured radiance responsivity was within the combined expanded uncertainty (k = 2) of the measurements. However, for most channels the agreement between the NPR and SIRCUS measurements was an order of magnitude better than the agreement between the Hardy and the SIRCUS measurements.

	$(C_{SIRCUS}-C_{source})/C_{SIRCUS}$ [%]		
Channel	NPR	Hardy (manf. RSRs)	Hardy (SIRCUS RSRs)
1	0.70	6.20	4.86
2	0.54	6.05	5.07
3	4.15	0.61	0.35
4	0.22	4.18	3.90
5	0.29	5.08	5.09
6	0.31	5.49	5.39
7	0.21	6.26	6.27
8	2.64	5.72	5.74

Table 2: Difference between measured and predicted signals from SimbadA measuring the NPR and the Hardy ISS.

3.2. Irradiance responsivity comparison

The cross-calibration technique consists of taking simultaneous direct solar measurements with two sun photometers. One sun photometer is a master instrument whose responsivity is well-known. The second sun photometer is an uncalibrated instrument, e.g.; a SimbadA radiometer. A roof-top calibration facility designed by the AERONET group at GSFC is used to cross-calibrate the CIMEL sun photometers that compose the network of automatic stations deployed around the world [2]. We use the same facility to cross calibrate the sun photometers that compose the SIMBIOS pool of instruments, including the SimbadA instruments.

The master sun photometers are calibrated in high altitude conditions at Mauna Loa Observatory (MLO, 3400 m) by the AERONET group [26] and then are deployed at the Goddard facility. Master instruments are calibrated on a three-month cycle while ensuring that one or two MLO calibrated instruments are at the GSFC facility.

The exoatmospheric voltages from the uncalibrated sun photometer are calculated relative to the ratio of the voltages from the master sun photometer,

$$V_0(\lambda_i) = V_0^{master}(\lambda_i)\frac{V(\lambda_i)}{V^{master}(\lambda_i)}, \tag{5}$$

where $V_0^{master}(\lambda_i)$ is the exo-atmospheric voltage for channel i of the master sun photometer. $V(\lambda_i)$ and $V^{master}(\lambda_i)$ are the signals measured respectively by the uncalibrated and the master sun photometers.

The band-center wavelengths of the SimbadA instrument channels are slightly different from any of those in the master instrument. The closest channel λ_j is then used in the calculations relative to the ratio of the voltages from the master sun photometer corrected from the Rayleigh scattering, the ozone absorption and the aerosol extinction:

$$\begin{aligned} V_0(\lambda_i) = V_0^{master}(\lambda_j)\frac{V(\lambda_i)}{V^{master}(\lambda_j)} * \exp\left[M(\theta_0) * \left(\tau_r(\lambda_i) - (\tau_r(\lambda_j)\right)\right] \\ * \exp\left[M(\theta_0) * \left(\tau_o(\lambda_i) - (\tau_o(\lambda_j)\right)\right] * \exp\left[M(\theta_0) * \tau_a(1\mu m)(\lambda_i^{-\alpha} - \lambda_j^{-\alpha})\right] \end{aligned} \tag{6}$$

where M is the airmass relative to the solar zenith angle q_0, t_R is the Rayleigh optical thickness, t_o is the ozone optical thickness, τ_a is the aerosol optical thickness, and α is the Angström exponent.

The exo-atmospheric voltages are calculated for pairs of measurements between the uncalibrated and the master sun photometers, usually taken within 30 s, though occasionally a time difference of 60 s is used to increase the number of occurrences. Data are taken for airmass less than 3 ($\theta_0 < 70^o$) to avoid extremely long atmospheric optical paths. The exo-atmospheric voltages of the uncalibrated instrument are then averaged and the variability is checked to ensure that the standard deviation of the mean value is less than 1 %.

Table 3 shows the results of the cross calibration of SIMBADA #09 radiometer relative to the master CIMEL sun photometer #89 performed on August 07 2002. The exo-atmospheric voltages retrieved through the day for three

channels (440 nm, 490 nm and 870 nm) are reported. The mean and standard deviation are shown in the last two lines of the table.

UTC Time	Time difference	Airmass	V_0 (DN) Chnl 1 (440 nm)	V_0 (DN) Chnl 2 (490 nm)	V_0 (DN) Chnl 3 (870 nm)
12.94	39.6	1.98	2317501	2960889	2246761
12.944	54	1.98	2319820	2954973	2235555
13.46	39.6	1.69	2308249	2946121	2242272
13.991	50.4	1.49	2289857	2925570	2208888
14.719	-28.8	1.3	2278436	2919725	2189098
14.736	28.8	1.3	2280716	2925570	2195675
15.138	14.4	1.23	2280716	2919725	2186910
15.142	28.8	1.23	2271611	2916807	2176002
15.197	-10.8	1.22	2276159	2919725	2191288
15.217	0	1.21	2280716	2922646	2193480
15.236	7.2	1.21	2278436	2916807	2180359
15.252	7.2	1.21	2285282	2928497	2197872
15.268	0	1.21	2273884	2916807	2184724
15.278	-18	1.21	2276159	2916807	2186910
15.294	-21.6	1.2	2285282	2922646	2197872
15.31	-21.6	1.2	2285282	2925570	2186910
Mean	**23 seconds**	----------	**2286757**	**2927430**	**2200036**
StDev	----------	----------	**0.66%**	**0.48%**	**1%**

Table 3: Typical exo-atmospheric coefficients of SimbadA #09 retrieved on August 7 2002 relative to master CIMEL sun photometer #89 for airmass lower than 3 and time difference shorter than 60 seconds.

In the fall of 2002, SIRCUS was used to determine the absolute spectral irradiance responsivity of the SimbadA instruments. Given an absolute exo-atmospheric solar irradiance, the SIRCUS measurements are used to predict the top of the atmosphere signal V_0according to:

$$V_o^{pred}(DN) = \int E(\lambda) s_E^i(\lambda) d\lambda, \quad (3)$$

where E(λ) is the exo-atmospheric solar irradiance, and $s_E^i(\lambda)$ is the SimbadA channel *i*'s absolute spectral irradiance responsivity. There are several different solar irradiance spectra to choose from. In Table 4, the differences between predicted V_0's using exo-atmospheric solar irradiance tables from Neckel and Labs [14], Wehrli [16], MODTRAN [15], and Thuillier, et al.[13], respectively, and measured values resulting from the cross-calibration at GSFC for Channels 1, 2 and 7 are shown.

			(*Vo* (measured)- *Vo* (predicted))/*Vo*(measured) [%]			
Channel	Center Wavelength	*Vo* Measured	Neckel and Labs (1984)	Wehrli (1986)	MODTRAN	Thuillier et al. (2002)
1	443.74	2.3033E+06	5.29	5.44	4.83	4.79
2	493.77	2.9403E+06	1.31	1.46	1.60	0.22
7	752.55	3.3100E+06	1.17	1.33	0.57	0.76

Table 4: Final measured *Vo* and predicted *Vo* calculated using exo-atmospheric solar irradiance spectra of Thuillier, Neckel and Labs, Wehrli and MODTRAN for SimbadA channels 1, 2 and 7.

A 1 to 2% difference between the predicted and measured V_0 is obtained for the 750 nm and 490 nm channels regardless of which solar irradiance table has been used for the calculation. At these two wavelengths, the best agreement comes from using the data from Thuillier, et al.[13]. Schmid, et al. [8] also found Thuillier gave the best overall agreement when comparing the different solar irradiance spectrums available for their calculation. However, the differences obtained for these two channels agree within the combined uncertainty of both calibration methods. A larger difference of about 5 % is obtained for the 440 nm channel and needs to be analyzed, although several explanations are possible. Two possible explanations involve interpolation, or the cross-calibration technique, both of which are more difficult at shorter wavelengths. This is to be studied in future work.

4. DISCUSSION

Correct description and understanding of aerosols is critical because of their direct and indirect radiative interaction with the atmosphere and their role in atmospheric correction algorithms [27]. Passive remote sensing at discrete wavelengths in networks such as AERONET yield values of aerosol optical depth (from downwelling solar irradiance) and information on the phase function, single-scattering albedo, complex index of refraction, and particle size distribution (from the angular distribution of sky radiance). The sensitivity of the derived parameters to the radiometric measurement uncertainty is complicated because of the nonlinearity of the retrieval process and the existence of additional effects such as reflected flux from the surface, pointing error, cloud screening, aerosol distributions, model assumptions, etc. The sensitivity analysis of Dubovik and co-workers assumed a wavelength independent uncertainty in total optical depth of 0.01 and an uncertainty in the sky radiance values of 5 %, based on AERONET. They found these uncertainties to be inadequate for the case of low optical depths [28]. In a separate study involving satellite measurements over ocean, differences of only a few tenths of a percent in the radiometric calibration compromised the accuracy of the aerosol optical depth determinations [29].

In this work, we have addressed the radiometric calibration uncertainty for solar irradiance measurements with sun photometers using a laboratory transfer approach (SIRCUS) that results in reduced uncertainties over previous laboratory approaches using lamp standards of spectral irradiance. Two of the three channels studied agreed with the cross-calibration procedure at GSFC to within 1.6 %, independent of the exo-atmospheric model. The 440 nm channel is discrepant, with differences of up to 5.4 %, leading to differences in optical depth that are greater than 0.02 for the air masses in Table 3. We also reported on the investigation of the accuracy of sky radiance measurements. We found a 1 % difference from the choice of the relative spectral responsivity (manufacturer vs. SIRCUS) and discrepancies of up to 6 % with the SIMBIOS calibration procedure using Hardy. These results would indicate the uncertainties assumed by Dubovik et al. for the radiometric calibration warrant further investigation.

Laboratory calibration of sun photometers is important for independent assessment of their stability as well as to assess the uncertainties and validity of the exo-atmospheric solar irradiance [8]. Detailed characterization and calibration of primary sun photometers using SIRCUS and other primary standard calibration facilities would produce additional comparison data and quantify other sources of error such as exact mapping of the field-of-view (important because of scattering within the baffle tube) and the temperature dependence of the radiometric responsivities (important because ambient temperature varies during field use). In addition, *in situ* field measurements with a stable radiometric source for a few key instruments would enable an assessment of the instrument repeatability. This procedure has been implemented with substantial benefit in ocean color research [30] and down-welling solar spectral irradiance networks [31].

Finally, reduced uncertainties in the Langley-Bouguer calibration combined with laboratory calibrations on SIRCUS of primary reference instruments may enable ground-based validation of airborne and space-based instruments such as the Solar Irradiance Monitor [32] that measure the exo-atmospheric solar irradiance.

ACKNOWLEDGEMENTS

We would like to acknowledge and thank James J. Butler and NASA's EOS Calibration/Validation program office for supporting NIST's efforts in this work and Thomas C. Larason for measurements of the out-of-band responsivity on the NIST Spectral Comparator Facility. We would also like to acknowledge the SIMBIOS project for providing the SimbadA from the SIMBIOS pool and Christian Verwaerde from the LOA for providing information on the instruments.

REFERENCES

1. Fargion, G.S., R.A. Barnes, and C.R. McClain, *In situ aerosol optical thickness collected by the SIMBIOS program (1997-2000): Protocols and data QC and analysis.* NASA/TM-2001-209982. 2001, Greenbelt, MD: NASA's Goddard Space Flight Center. 103.
2. Holben, B.N., et al., *Aeronet - a federated instrument network and data archive for aerosol characterization.* Remote Sens. Environ., 1998. **66**: p. 1-16.
3. SIMBIOS, *http://simbios.gsfc.nasa.gov*. 2003.
4. WRC, *http://www.pmodwrc.ch*. 2003.
5. RCF, *http://spectral.gsfc.nasa.gov/*. 2003.
6. Pietras, C., et al., *Calibration of sun photometers and sky radiance sensors*, in *In situ aerosol optical thickness collected by the SIMBIOS program (1997-2000): protocols, and data QC and analysis*, R.B. G. S. Fargion, and C. McClain, Editor. 2001, NASA's Goddard Space Flight Center: Greenbelt, MD.
7. Meister, G., et al., *The First SIMBIOS Radiometric Intercomparison (SIMRIC-1), April--September 2001*. NASA/TM 2002--210006. 2002, Greenbelt, MD: NASA Goddard Space Flight Center. 60.
8. Schmid, B., et al., *Evaluation of the applicability of solar and lamp radiometric calibrations of a precision sun photometer operating between 300 and 1025 nm.* Applied Optics, 1998. **37**: p. 3923-3941.
9. Wehrli, C., *Calibrations of filter radiometers for determination of atmospheric optical depth.* Metrologia, 2000. **37**: p. 419-422.
10. Brown, S.W., G.P. Eppeldauer, and K.R. Lykke, *NIST facility for Spectral Irradiance and Radiance Responsivity Calibrations with Uniform Sources.* Metrologia, 2000. **37**: p. 579-582.
11. Eppeldauer, G.P., et al., *Realization of a spectral radiance responsivity scale with a laser-based source and Si radiance meters.* Metrologia, 2000: p. 531-534.
12. Brown, S.W. and B.C. Johnson, *A portable integrating sphere source for radiometric calibrations from the visible to the shortwave infrared.* The Earth Observer, 1999. **11**(3): p. 14-19.
13. Thuillier, G., et al., *The solar spectral irradiance from 200 to 2400 nm as measured by the SOLSPEC spectrometer from the ATLAS and EURECA missions.* Sol. Phys., 2003. **214**: p. 1-22.
14. Neckel, H. and D. Labs, *The solar radiation between 3300 and 12500 A.* Sol. Phys., 1984. **90**: p. 205-258.
15. Berk, A., Bernstein, L.S., Robertson, D.C., *"MODTRAN: A Moderate Resolution Model for LOWTRAN 7"*, GL-TR-89-0122, 1989.
16. Wehrli, C., *Extraterrestrial solar spectrum*. Publ. 615. 1985, Davos-Dorf, Switzerland: Physikalisch-Meterologisches Observatorium Davos and World Radiation Center.
17. Eppeldauer, G.P. and D.C. Lynch, *Opto-mechanical and electronic design of a tunnel-trap Si- radiometer.* J. Res. NIST, 2000. **105**(6): p. 813-828.
18. Fowler, J. and M. Litorja, *Geometric area measurements of circular apertures for radiometry at NIST.* Metrologia, 2003. **40**: p. S9-S12.
19. Yoon, H.W., et al. *Temperature scales using radiation thermometers calibrated from absolute irradiance and radiance responsivity*. in *2003 NCSL International Workshop and Symposium*. 2003. Orlando, FL.
20. Marketon, J., et al., *A filter radiometer monitoring system for integrating sphere sources.* SPIE Proc., 2001. **4169**: p. 260-265.
21. Walker, J.H., et al., *Spectral Irradiance Calibrations*. NBS Special Publication 250-20. 1987, Gaithersburg MD: U.S. Department of Commerce. 37 pages plus appendices.
22. Larason, T.C., S.S. Bruce, and A.C. Parr, *Spectroradiometric detector measurements: Part I--Ultraviolet detectors and Part II--Visible to near-infrared detectors*. NIST Special Publication 250-41. 1998, Gaithersburg MD: U.S. Department of Commerce. 84 pages plus appendices.
23. Johnson, B.C., et al., *Comparison of cryogenic radiometry and thermal radiometry calibrations at NIST using multichannel filter radiometers.* Metrologia, 2003. **40**: p. S216-S218.
24. Butler, J.J., B.C. Johnson, and R.A. Barnes, *Radiometric measurement comparisons at NASA's Goddard Space Flight Center: Part I. The GSFC sphere sources.* The Earth Observer, 2002. **14**(3): p. 3-8.
25. Butler, J.J., B.C. Johnson, and R.A. Barnes, *Radiometric measurement comparisons at NASA's Goddard Space Flight Center: Part II. Irradiance lamp comparisons and the NIST sphere source.* The Earth Observer, 2002. **14**(4): p. 25-29.
26. Holben, B.N., et al., *An emerging ground-based aerosol climatology: Aerosol Optical Depth from AERONET.* J. Geophys. Res., 2001. **106**: p. 12 067-12 097.

27. USCCSP, *http://www.climatescience.gov*.
28. Dubovik, O., et al., *Accuracy assessments of aerosol optical properties retrieved from Aerosol Robotic Network (AERONET) sun and sky radiance measurements.* J. Geophys. Res., 2000. **105**: p. 9791-9806.
29. Mishchenko, et al., *Aerosol retrievals over the ocean by use of channels 1 and 2 AVHRR data: sensitivity analysis and preliminary results.* Applied Optics, 1999. **38**: p. 7325-7341.
30. Hooker, S.B. and J. Aiken, *Calibration evaluation and radiometric testing of field radiometers with the SeaWiFS Quality Monitor (SQM).* Journal of Atmospheric and Oceanic Technology, 1998. **15**: p. 995-1007.
31. Early, E.A., E.A. Thompson, and P. Disterhoft, *Field calibration unit for ultraviolet spectroradiometers.* Applied Optics, 1998. **37**: p. 6664-6670.
32. *Solar Irradiance Monitor: http://lasp.colorado.edu/sorce/sim.html*. 2003.